The atomic diffusion process in Al-Mn superlattices examined by annealing treatments

1989 J. Phys.: Condens. Matter 1 7303

(http://iopscience.iop.org/0953-8984/1/40/005)

J. Phys.: Condens. Matter **1** (1989) 7303–7308. Printed in the UK

The atomic diffusion process in Al–Mn superlattices examined by annealing treatments

Y Nishihata†, M Nakayama‡, N Sano† and H Terauchi†
† School of Science, Kwansei Gakuin University, Nishinomiya 662, Japan
‡ Department of Applied Physics, Osaka City University, Sumiyoshi-ku, Osaka 558, Japan

Received 16 March 1989

Abstract. The annealing process of superlattices with alternating Al and Mn layers has been examined by x-ray diffraction. The time dependence of structural relaxation cannot be explained by a single relaxation time, but it follows the Kohlrausch relaxation law, $\exp[-(t/\tau)^{\beta}]$, where the parameters β and τ are dependent on the annealing temperature. The value of β increases almost linearly with increasing annealing temperature, and the temperature dependence of τ is satisfied by the Arrhenius equation. It reflects the competition between several atomic diffusion processes.

1. Introduction

Annealing experiments of artificial superlattices have great interest from the viewpoint of growth kinetics of new phases. It has been known that anneals of the superlattices produce reaction of the layers to form crystalline phases predicted by the equilibrium diagram [1] or even amorphous phases [2–4]. Not all of the compound phases were observed to be present simultaneously during the annealing process. A model was proposed to describe the thin-film alloy formation [5, 6]. It is postulated in the model that the intermediate compound layers have specific crystal structures corresponding to the concentration, and the interface compositions are constant throughout the time of growth, independent of the layer thickness. The growth kinetics are subject to a combination of two types of processes, the diffusion of matter and the rearrangement of the atoms. It is termed diffusion controlled when the former process or interface controlled when the latter process is dominant. The system in which the alloys have the same crystal structure over the whole concentration range has no competition in the atomic rearrangement process; that is, the atomic interdiffusion occurs without changing the crystal structure. For example, such a competition can be nearly ignored in the case of the Au–Ag superlattice, as reported by Cook and Hilliard [7], because the structure of Au and Ag are both face-centred cubic (FCC) and all Au–Ag alloys have the same crystal structure [8]. Since they prepared alternating layers of metals to study the problem of spinodal decomposition and diffusion in metals in cubic lattices, our case is beyond the scope of their works. In this paper, the annealing process for Al–Mn superlattices are described, where multiple atomic rearrangement processes are competing during the annealing.

2. Experiment

Superlattices with alternating Al and Mn layers have been grown by molecular-beam epitaxy (MBE) [9, 10]. In the superlattice crystals Mn atoms form an FCC lattice (γ-phase)

0953-8984/89/407303 + 06 $02.50

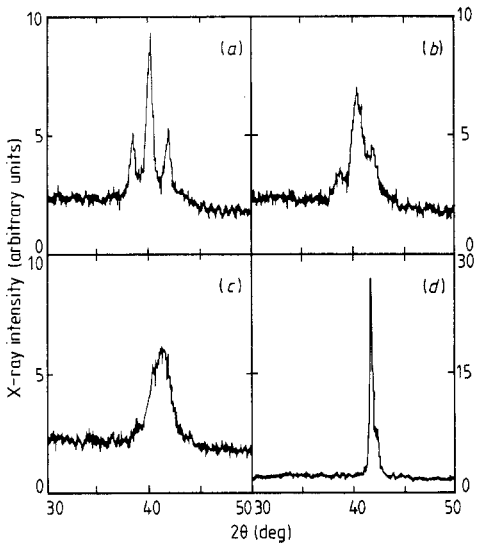

Figure 1. X-ray diffraction profiles near the Al and Mn (111) reflection of $[Al(50\ Å)|Mn(8\ Å)]_{80}$ grown on a glass substrate during the annealing process at 300 °C: (*a*) before annealing, (*b*) after annealing for 7 min, (*c*) after annealing for 15 min, (*d*) after annealing for 5 min at 700 °C.

at room temperature when the layer thickness is less than a critical thickness of about 30 Å. The synthesis of an Al(FCC)–Mn(FCC) superlattice has been achieved, where there is a little lattice strain between the Al and Mn layers. The detailed growth conditions are the same as described in [9]. The superlattice crystals were made on room-temperature quartz glass plates. The absence of sharp Bragg reflections from the glass substrate enabled us to observe weak reflections from the samples. The samples grown on glass plates have a preferred orientation with [111] along the growth direction.

X-ray diffraction experiments were carried out using a double-axis diffractometer. Cu Kα radiation monochromatised by a pyrolytic graphite crystal was employed as the x-ray source. The x-ray intensity was measured using a position-sensitive proportional counter (PSPC). To study diffusion, the samples in a vacuum of about 10^{-3} Torr were heated to 200, 300, 350, 400, 450, 500 °C, and higher temperatures by irradiation with infrared rays. The temperature was monitored with a thermocouple that was in direct contact with the irradiated surface of the sample. The annealing temperature was controlled to ±5 °C. It took only a few seconds to heat up the sample. The time dependence of the diffraction profiles has been observed *in situ*. That is, the sample temperature was changed suddenly to the annealing temperature and the diffraction profiles were consecutively observed. One diffraction pattern can be obtained in 10 to 30 s.

3. Result and discussion

Figure 1 shows the x-ray diffraction pattern of $[Al(50\ Å)|Mn(8\ Å)]_{80}$ grown on a glass substrate during the annealing process at 300 °C. X-ray profiles from Al–Mn superlattices were observed using a PSPC. Since the angular precision of the PSPC is rather poor, it is difficult to detect the small angle shift. Figure 1(*a*) is the diffraction pattern around the Al and Mn (111) reflection for the unannealed sample. As is shown in figure 1(*b*), the Al and Mn (111) reflection and the first-order satellites shift towards higher angles after annealing for 7 min at 300 °C. This indicates that the lattice is compressed due to alloying. After annealing for a little more time at the same temperature the reflections shift further

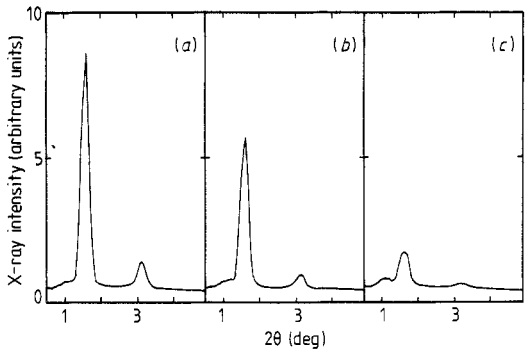

Figure 2. Small-angle x-ray diffraction profiles of $[Al(50\,Å)|Mn(8\,Å)]_{80}$ grown on a glass substrate during the annealing process at 350 °C: (*a*) before annealing, (*b*) after annealing for 10 min, (*c*) after annealing for 2 h.

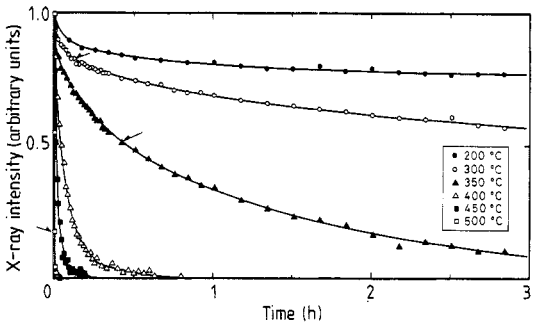

Figure 3. Time dependence of the integrated intensity of the first peak in the small-angle range ($Q_0 = 0.108\,Å^{-1}$). The arrows represent the time when the satellite peaks around the Al–Mn (111) reflection disappeared: after annealing for 8 min at 300 °C, 25 min at 350 °C, 30 s at 500 °C.

and their intensities decrease. Instead a broad peak which corresponds to Al_6Mn (222) appears, as shown in figure 1(*c*). At this time the domain size of the Al–Mn alloy in the direction normal to the plane is roughly estimated to be 30 Å using the Scherrer equation. On annealing for more time or at higher temperatures the peak intensity increases and becomes sharp. Figure 1(*d*) shows the diffraction pattern after annealing for 5 min more at 700 °C. The peak width becomes close to the limit of instrumental resolution. Other reflections from the alloy are not observed by 2θ–θ scanning, implying that the domains of the alloy are oriented well in the direction normal to the growing plane. Sharpening of the rocking curve was also found. Figure 2 shows the x-ray diffraction profiles in the small-angle region for the same structure during the annealing process at 350 °C. Figure 2(*a*) is the profile from the unannealed sample. Figures 2(*b*) and 2(*c*) are the profiles after annealing for 10 min and 2 h, respectively. Figure 3 shows the time dependence of the integrated intensity of the first peak of the small-angle scattering ($Q_0 = 0.108\,Å^{-1}$) for each annealing temperature. Arrows indicate the time when the satellite peaks around the Al–Mn (111) reflection disappeared and only the reflection of the alloy remained in the wide-angle range. X-ray diffraction profiles in the wide-angle range were observed at 200, 300, 350 and 500 °C. As the annealing temperature becomes higher and higher, satellite peaks around the Al–Mn (111) reflection can be observed until the proportion of the small-angle peak intensity is smaller and smaller. In the case of the annealing treatment at 200 °C, the satellite peak intensity around the Al–Mn (111) reflection hardly changed despite the diminution of the first peak intensity in the small-angle range. The disappearance of the satellite peaks around the Al–Mn (111) reflection is interpreted as the vanishing of structural coherency due to the alloying. The modulation structure may be described by a Fourier sum in real space. If the diffusion constant is independent of the concentration, a solution of Fick's second law leads to the following time dependence of the Fourier amplitude $q(t)$, namely, Debye relaxation [11]:

$$q(t) = q_0 \exp(-t/\tau) \tag{1}$$

where τ is the time constant, which may be determined through the temperature

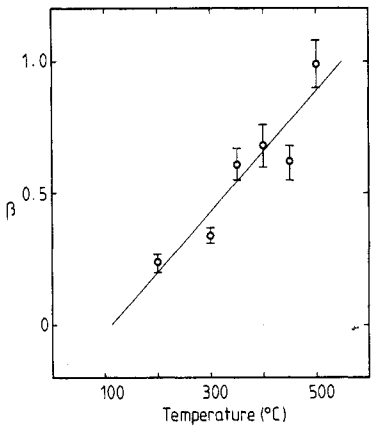

Figure 4. Temperature dependence of parameter β.

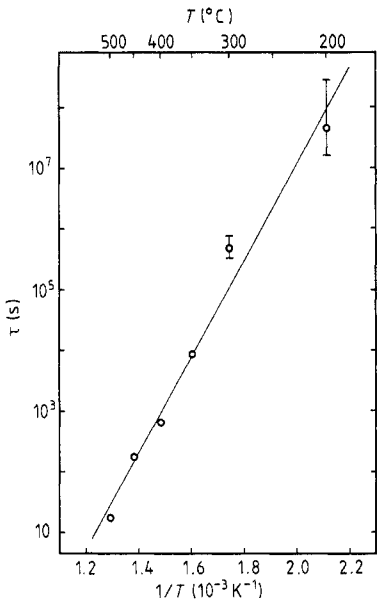

Figure 5. Arrhenius plot of τ.

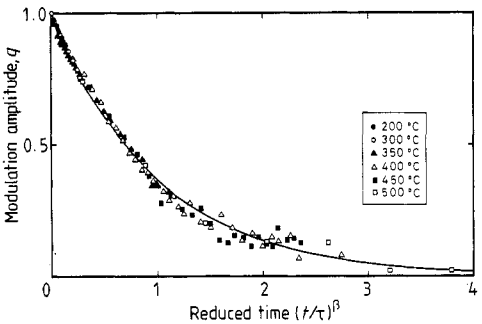

Figure 6. Plots of the first term in the Fourier series of mass-density modulation with respect to the scaled time. They fall on a universal curve represented by the full curve, $\exp[-(t/\tau)^{\beta}]$, irrespective of the annealing temperature.

dependence of the diffusion constant. However, the time dependence of the square root of the integrated intensity, $q(t)$ cannot be explained by a single relaxation time τ. We found that it follows the Kohlrausch anomalous relaxation law [12], which postulates a statistical distribution of relaxation time:

$$q(t) = q_0 \exp[-(t/\tau)^{\beta}] \qquad \text{with } 0 \leqslant \beta \leqslant 1. \tag{2}$$

In calculating the parameters β and τ, first the value of τ was determined by a least-square method with a given initial value of β. The pairs of β and τ which reduce the mean square error to a minimum were consequently chosen. It was found that parameters β and τ were dependent on the annealing temperature. As is shown in figure 4, the value of β increases almost linearly with increasing temperature and it becomes about 1 at 500 °C, implying that $q(t)$ obeys the Debye relaxation then. At room temperature the value of β is very small; this indicates that the superlattice structure is very stable since $q(t)$ is almost a constant value. When one postulates a relation $\beta = (T - T_0)/\Delta$ the values of the parameters T_0 and Δ are obtained from the data shown in figure 4: $T_0 =$ 390 K and $\Delta = 430$ K. Figure 5 represents an Arrhenius plot of τ . The temperature

dependence of τ fits satisfactorily to an Arrhenius equation, $\tau = \tau_0 \exp(E/kT)$, though we do not have any rigorous theoretical background at present. The activation energy E is about 1.6 eV. Figure 6 shows plots of the first term in the Fourier series, $q(t)$, for each annealing temperature with respect to the scaled time $(t/\tau)^{\beta}$. They fall on a universal curve irrespective of the annealing temperature.

Kohlrausch's relaxation law is found in a very wide range of phenomena and materials [12–15]. It has been speculated that many complex systems with highly degenerate and locally stable states exhibit an ultrametric topology [13]. Kinetic models in ultrametric spaces that describe hierarchical patterns of energy barriers lead to equation (2) [14]. Figure 3 suggests that structural coherency of the superlattice is maintained at the initial stage of annealing process although atomic interdiffusion advances the alloying. It seems that the lattice coherency between layers can be destroyed by changing the atomic arrangement of FCC to that of the alloy phase because of the difference between FCC structure and alloy structure. Satellite peaks around Bragg reflections in the wide-angle range are sensitive to the goodness of crystalline and lattice coherency, while small-angle scatterings are not so sensitive to them. On annealing at 300 °C, the intensity of satellites around the Al–Mn (111) reflection disappeared completely when the integrated intensity of the small-angle scattering was reduced by only 20% of the initial intensity, as indicated by the arrow in the figure. The result of the annealing at 300 °C also suggests that a small amount of atoms intruding into next layer can destroy the FCC lattice above a certain temperature. On the other hand, it is surprising that on annealing at 500 °C the structural coherency of the FCC lattice is maintained until the x-ray intensity of the first peak in the small-angle range is reduced to about 20% of the initial intensity. The conflicting time dependences between the intensity of the small-angle scattering and that of the wide-angle scattering suggest that there are several atomic rearrangement processes, namely, one process where the original lattice structure is maintained and another process where the FCC structure is transformed into the alloy structure, and that the latter process was suppressed relatively at higher temperatures. In other words, the problem is whether one atom and the local environment prefers an FCC structure or the alloy structure under the structural coherency of the FCC lattice. The FCC structure is stable from the viewpoint of the coherency of Al(FCC)–Mn(FCC) superlattice, while the alloy structure is stable from the viewpoint of the concentration ratio of Al and Mn. Diffusing atoms have the frustration to make their local structure because either structure may be possible locally. The time evolution of the system can be represented by a hierarchical tree in an ultrametric space [15]. When the atoms in each sublayer are assigned numbers according to their local structures, we can consider the system of the superlattice just as spins. The top level of the hierarchical tree corresponds to the initial state, that is, all atoms have the FCC structure locally. The ordering or the status of the system evolves by temperature-assisted hopping with potential barrier Δ. If diffusing atoms have two possible local structures, the time dependence of the order parameter of the superlattice period may not be explained by a single relaxation time, but it can follow the Kohlrausch relaxation law having a statistical distribution of relaxation time. Kinetic models in an ultrametric space predict that the parameter β is proportional to the absolute temperature T. But we must introduce a critical temperature T_0 experimentally so as to represent the parameter β by a linear equation with respect to T. The intensity of the satellite peaks around Al–Mn (111) did not change very much after annealing for 3 h at 200 °C. But some structural transformation may occur after longer annealing treatment. The equilibrium diagram permits a very small amount of solid solution of Al (Mn) atom in Mn (Al) without changing their crystal structures [16],

implying that the process of structural transformation as a result of atomic interdiffusion will be suppressed at sufficiently low temperature and in low concentration of the other constituent. Such a small amount of atomic diffusion can contribute to reducing the x-ray intensity in a small-angle region without changing the crystal structure. It seems that the mechanism is one of several factors that determine the temperature T_0 and contribute to the stability of artificial superlattices.

4. Conclusion

The diffusion process of Al–Mn superlattices has been examined by annealing treatment. The compression of the sample has been observed. The alloys are well oriented in the direction normal to the film and have larger domain size than the unannealed sample. It was found that mass–density modulation was destroyed in accordance with the Kohlrausch relaxation law, $\exp[-(t/\tau)\beta]$. The parameters β and τ are dependent on annealing temperature. Above a certain temperature T_0, the value of β increases almost linearly with increasing annealing temperature, as predicted by a kinetic model in an ultrametric space, while the temperature dependence of τ can be fitted to an Arrhenius equation. The competition between several kinds of local structures, namely, FCC and alloy structures, can explain the atomic diffusion process. The scaling of data for each annealing temperature means that atomic interdiffusion and structural transformation are subjected to the same mechanism over a wide temperature range.

References

[1] Ottaviani G 1979 *J. Vac. Sci. Technol.* **16** 1112
[2] Schwarz R B and Johnson W L 1983 *Phys. Rev. Lett.* **51** 415
[3] Van Rossum M, Nicolet M-A and Johnson W L 1984 *Phys. Rev.* B **29** 5498
[4] Clemens B M 1986 *Phys. Rev.* B **33** 7615
[5] Kidson G V 1961 *J. Nucl. Mater.* **3** 21
[6] Gösele U and Tu K N 1982 *J. Appl. Phys.* **53** 3252
[7] Cook H E and Hilliard J E 1969 *J. Appl. Phys.* **40** 2191
[8] Hansen M 1958 *Constitution of Binary Alloys* 2nd edn (New York: McGraw-Hill) p 5
[9] Nishihata Y, Nakayama M, Sano N and Terauchi H 1988 *J. Appl. Phys.* **63** 319
[10] Nishihata Y, Nakayama M, Sano N and Terauchi H 1988 *Trans. Japan. Inst. Met. Suppl.* **29** 489
[11] Fleming R M, McWhan D B, Gossard A C, Wiegmann W and Logan R A 1980 *J. Appl. Phys.* **51** 357
[12] Palmer R G, Stein D L, Abrahams E and Anderson P W 1984 *Phys. Rev. Lett.* **53** 958
[13] Mézard M, Parisi G, Sourlas N, Toulouse G and Virasoro M 1984 *Phys. Rev. Lett.* **52** 1156
[14] Ogielski A T and Stein D L 1985 *Phys. Rev. Lett.* **55** 1634
[15] Rammal R, Toulouse G and Virasoro M A 1986 *Rev. Mod. Phys.* **58** 765
[16] Hansen M 1958 *Constitution of Binary Alloys* 2nd edn (New York: McGraw-Hill) p 110